

Design and Modeling of Metamorphic Dual-Junction InGaP/GaAs Solar Cells on Si Substrate for Concentrated Photovoltaic Application

Nikhil Jain, *Student Member, IEEE*, and Mantu K. Hudait, *Senior Member, IEEE*

Abstract—We have investigated the concentrated photovoltaic performance of metamorphic monolithic InGaP/GaAs dual-junction (2-J) solar cells on Si substrate under AM1.5d spectrum using finite-element analysis. The current-matching condition between each subcell was realized for threading dislocation density varying from 10^5 to 10^7 cm^{-2} , emanating from the mismatch between GaAs and Si substrate. Through comprehensive cell design and by mitigating the losses due to shadowing effect and series resistance, we present an optimal cell design for harnessing the maximum potential of 2-J InGaP/GaAs cell integrated on Si substrate for concentrated photovoltaics. The optimization of front grid spacing and sheet resistance of the window layer were the key design parameters taken into consideration for extending the peak performance toward higher concentrations. Finally, we present an optimized 2-J InGaP/GaAs cell design on Si, which exhibited a theoretical conversion efficiency of 33.11% at 600 suns at a realistic TDD of 10^6 cm^{-2} , indicating a promising future for integrating III–V cell technology on Si for low-cost concentrated photovoltaics.

Index Terms—Grid design, photovoltaic cells, semiconductor device modeling, III–V on Si, III–V semiconductor materials.

I. INTRODUCTION

MULTIJUNCTION III–V compound semiconductor solar cells have been the dominant choice for space applications; however, their expensive cost has limited their application for the terrestrial sector. Concentrated photovoltaic (CPV) systems utilizing III–V multijunction cells provide a great promise for delivering electrical power at lower cost than traditional flat-plate systems [1]. Under high sun concentration, the concentrator begins to dominate the overall system cost as the cell size becomes much smaller and the economics becomes strongly influenced by the efficiency–concentration relationship. The relatively small cell size reduces the amount of material and, consequently, the system cost.

Most of the III–V solar cells utilized in CPV systems are grown on either GaAs or Ge substrate, both of which are not only smaller in diameter, but are also more expensive than Si. Direct integration of III–V semiconductors on large diameter, cheaper, and readily available Si substrate is highly desirable for increased density, low-cost, and lightweight photovoltaics.

Manuscript received July 3, 2013; accepted August 17, 2014. This work was supported in part by the Institute for Critical Technology and Applied Sciences, Virginia Tech.

The authors are with the Advanced Devices and Sustainable Energy Laboratory, Department of Electrical and Computer Engineering, Virginia Tech, Blacksburg, VA 24061 USA (e-mail: jain34@vt.edu; mantu@vt.edu).

Color versions of one or more of the figures in this paper are available online at <http://ieeexplore.ieee.org>.

Digital Object Identifier 10.1109/JPHOTOV.2014.2351619

III–V integration on Si unifies the excellent optical properties of III–V materials with the volume manufacturability of Si, allowing a path for significantly driving down the cost. Furthermore, III–V on Si technology is also attractive for integration with commercially available substrate reuse techniques such as spalling [2] and epitaxial lift-off [3]–[5] to explore additional cost saving schemes. The approach of direct GaAs on Si epitaxy could be extended to record efficiency 3-J solar cells that utilize dilute nitride cell [6] as well as with the state-of-the-art inverted metamorphic solar cells [7]. However, polar on nonpolar epitaxy, thermal mismatch, and 4% lattice-mismatch make the growth of GaAs on Si challenging, rendering the metamorphic solar cell sensitive to dislocations.

We have recently modeled a 2-J InGaP/GaAs cell on Si with a theoretical efficiency greater than 29% (1-sun) at a threading dislocation density (TDD) of 10^6 cm^{-2} by carefully engineering the cell design and by realizing the current-matching condition taking into account the TDD [8], [9]. Experimental 2-J InGaP/(In)GaAs-based solar cells have been an integral part of most of the high efficiency multijunction solar cells [6], [7], [10], [11]. The highest 1-sun efficiency reported for monolithic 2-J InGaP/GaAs cell on Si is 18.6% [12]. There has not been significant experimental or theoretical work done on the monolithic integration of 2-J InGaP/GaAs solar cells on Si for operation under concentrated sunlight, which takes into account the impact of TDD. To the best of our knowledge, this paper provides the first simulation study on the CPV performance of metamorphic 2-J InGaP/GaAs solar cells on Si substrate which takes into account the impact of TDD using finite element analysis [13]. The results from our study will be useful for future design and optimization of metamorphic 3 J and beyond III–V solar cells on Si substrate.

II. THEORY AND MODELING PROCESS

In CPV systems, lenses focus the sunlight onto a small area cell, enabling higher efficiency under concentrated sunlight. Typically, the current density of a solar cell is proportional to the intensity of the incident light and inversely proportional to the cell area. The efficiency increases with the concentration until series resistance or cell heating begins to limit the performance. For lattice-matched 2-J InGaP/GaAs cells, an absolute 4% drop in efficiency was observed for the cell operating at ~ 100 °C compared with ~ 25 °C [14]. However, extremely small 2-J cells (0.36 mm^2) have been previously used under ~ 1000 x concentration without employing heat sinks for passive cooling [3]. Since we have utilized small cell dimensions (≤ 0.25 mm^2)

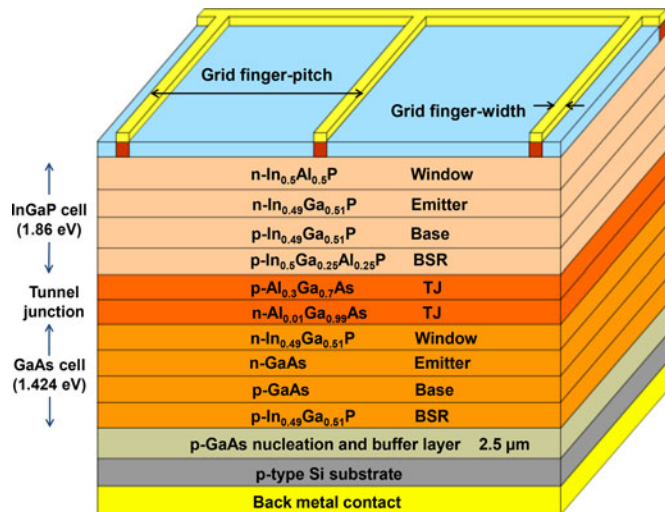


Fig. 1. Schematic depiction of 2-J InGaP/GaAs solar cell on Si.

in our model, we neglected the cell heating under concentrated sunlight for our prototype cells.

A. Concentrated Photovoltaic Design Consideration for Metamorphic III–V Solar Cells on Si

The most important design aspects for maximizing the CPV performance of multijunction solar cells include the 1) realization of current-matching, 2) optimization of the design tradeoffs between the front metal shadowing and the series resistance, and 3) proper tunnel-junction design. An additional aspect that becomes extremely important for designing metamorphic tandem cells for CPV is the optimization of all these parameters taking into account the impact of TDD.

In this paper, we have utilized our calibrated model for 2-J InGaP/GaAs cell on Si under AM1.5 g [9] as the first step. The entire structure is metamorphic with respect to Si substrate. However, the III–V subcells are internally lattice matched. Although, the InGaP subcell was lattice matched to the bottom GaAs subcell, all the threading dislocations (TDs) generated due to the mismatch between GaAs and Si were assumed to propagate into the top InGaP subcell. We utilized the same material and device parameters, namely, band gaps, minority carrier mobility and lifetimes, diffusion coefficients, and surface recombination velocities [9], [15]–[21] to evaluate the CPV performance under AM1.5 d (900 W/m²). Utilizing an incident power density of 1000 W/m² would only alter the efficiency and not affect any of the other solar cell parameters. The schematic of the 2-J InGaP/GaAs cell structure on Si is shown in Fig. 1. The grid finger-pitch was defined as the end-to-end distance between two adjacent fingers, each being 2- μ m wide.

B. Tunnel Junction Design Under Concentrated Sunlight

The tunnel junctions (TJs) may limit the overall performance if the current density of the solar cell exceeds the peak tunneling current density (J_{T-Peak}) of the TJ. However, it is extremely challenging to estimate the carrier lifetimes in the heavily doped

TJs at a given TDD. Therefore, for the simplification of our analysis, the AlGaAs/GaAs TJ in our cell structure was assumed to be unaffected at a TDD of 10⁶ cm⁻². The potential risk of reduction in J_{T-Peak} due to TDD can be mitigated by utilizing AlGaAs/GaAs quantum-well TJs, which have J_{T-Peak} over 300 A/cm², equivalent to operation under 20 000 suns [22].

C. Series Resistance Losses During Grid Design

Typically, the degradation in cell performance under high concentration due to series resistance is attributed to the 1) shadowing losses due to front grid obscuration, 2) resistance of the epitaxial layers including the sheet resistance of the window-emitter layers, 3) contact resistance at the metal–semiconductor interface, and 4) resistivity of the metal gridlines. Selecting an appropriate metal stack and the annealing condition during the cell fabrication can minimize the contribution from the latter two factors. Major contributions to the power loss due to series resistance can be attributed to the shadowing of the metal fingers as well as the emitter sheet resistance [23]. The optimization of these specific parameters is, therefore, extensively addressed in this study.

There have been several methods proposed for characterizing the series resistance of a solar cell [24]–[28]. Most of the methods are based on computing slopes and may require current–voltage (I – V) measurements at multiple concentration [27] or both light and dark I – V measurements [25], [26]. Although, the most commonly used methods are based on computing the slope near the V_{oc} , these methods are sensitive to the point considered on the characteristic curve. To compute series resistance, we have utilized the method proposed by Araujo and Sanchez [24], where the overall contribution of the series resistance is considered as an effective series resistance, R_s and is calculated by evaluating numerically the area, A , under the light I – V curve of the solar cell [24] using

$$R_s = 2 \left[\frac{V_{oc}}{I_{sc}} - \frac{A}{I_{sc}^2} - n \frac{kT}{q} \frac{1}{I_{sc}} \right] \quad (1)$$

where n is the effective ideality factor of the diode, and k is the Boltzmann constant. This method of computing the area is superior to computing the slope as this method smoothens the experimental data errors rather than enhancing the noise.

III. RESULTS AND DISCUSSION

A. Current-Matching in 2-J InGaP/GaAs Solar Cell on Si

In our device structure, owing to the lattice-mismatch between GaAs and Si, the TDs may propagate into the active junctions and serve as recombination centers for electron and holes, leading to degradation in the minority carrier lifetimes and, thus, the cell performance. In our model, the maximum minority electron lifetime (τ_n) in lattice-matched p-type GaAs and p-type InGaP base were considered to be 20 [15], [16] and 10 ns [20], [21], respectively. Due to the lattice-mismatch between GaAs and Si, τ_n in p-type GaAs and p-type InGaP base were estimated to be 1.49 and 3.17 ns, respectively, at a TDD of 10⁶ cm⁻² [9]. Carefully taking into account the impact of

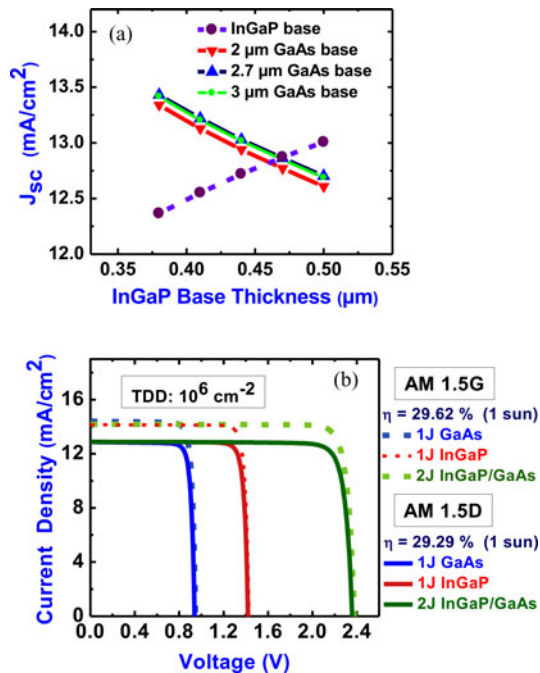


Fig. 2. (a) Short-circuit current density as a function of variation in the base thickness of the InGaP subcell to realize current-matching at a TDD of 10^6 cm^{-2} under AM1.5 d. (b) Current-matched J - V characteristic of 2-J InGaP/GaAs solar cell on Si under AM1.5 g (dashed curves) and AM1.5 d (solid curves) spectrum.

these degraded lifetimes on the cell performance, we achieved the current-matching condition between the two subcells under AM1.5 d spectrum utilizing a similar method as outlined earlier [9]. Owing to the spectral differences between AM1.5 g and AM1.5 d spectra, for the same current-matched design under AM1.5 g ($2\text{-}\mu\text{m}$ thick p-GaAs and $0.38\text{-}\mu\text{m}$ -thick p-InGaP base), the J_{sc} in the GaAs subcell was found to be 7.66% higher than the top InGaP subcell under AM1.5 d spectrum.

Our preliminary 2-J InGaP/GaAs cell structure on Si employed a grid finger-pitch of $500 \mu\text{m}$. In order to maximize the J_{sc} of our 2-J InGaP/GaAs cell and to achieve the current-matching condition under AM1.5 d at a TDD of 10^6 cm^{-2} , the thicknesses of individual layers in both the subcells were optimized as shown in the Fig. 2(a). The optimal p-GaAs base thickness was found to be $2.7 \mu\text{m}$, beyond which the minority carriers could not be efficiently collected as a consequence of the reduced electron lifetime owing to the dislocations in the p-GaAs base. The optimal thicknesses for the p-InGaP base was found to be $0.47 \mu\text{m}$, which allowed to extract the maximum current density from the bottom current-limiting GaAs subcell, while still maintaining the current-matching condition. This current-matched 2-J InGaP/GaAs cell design on Si exhibited an efficiency of 29.29% under AM1.5 d (1-sun) with a J_{sc} of $12.86 \text{ mA}/\text{cm}^2$ as indicated by the solid curves in Fig. 2(b). The contribution of individual GaAs and InGaP subcells towards the 29.29% efficiency were 11.44% and 17.85%, respectively, and the V_{oc} of the GaAs and InGaP subcells were 0.94 V and 1.42 V, respectively. The corresponding band gap-voltage offset, $W_{oc} (= E_g/q - V_{oc})$ for the GaAs and InGaP subcells were

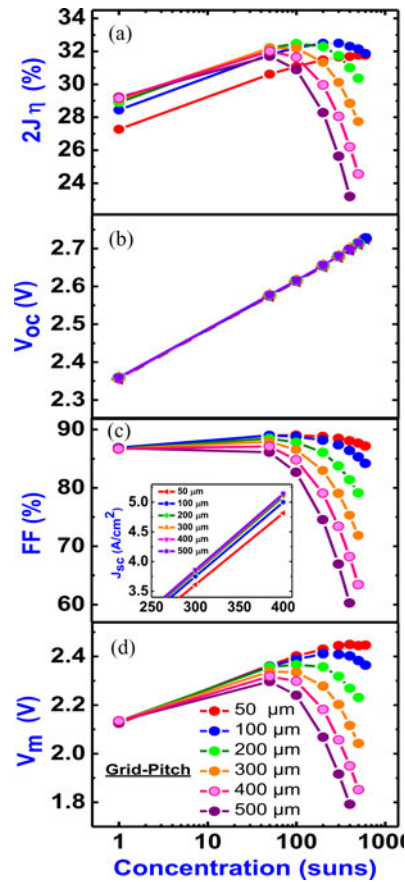


Fig. 3. Impact of concentration on the performance of 2-J InGaP/GaAs cell on Si: (a) η , (b) V_{oc} , (c) FF (inset shows J_{sc}), and (d) V_m for various grid finger-pitches under AM1.5 d spectrum at a TDD of 10^6 cm^{-2} .

calculated to be 0.48 V and 0.44 V, respectively. These values of W_{oc} higher than the ideal W_{oc} value of ~ 0.4 V [10] were indicative of the dominance of nonradiative recombination in the base of both the subcells owing to the TDs.

B. Optimization of Spacing Between Grid Fingers

The performance of III-V solar cells for CPV operation can be significantly impacted if the front grid design is not optimized for a specific target concentration. Lowering the grid separation between the front gridlines (or increasing the grid shadowing) improves the I^2R resistive losses, but at the same time reduces the photon flux that reaches the cell and in turn limits the J_{sc} . Thus, there are design tradeoffs between the shadowing effect and the series resistance which needs to be optimized to enable the best performance under a specific target concentration.

In order to optimize the losses due to shadowing effect and series resistance, we varied the grid finger-pitch from 500 to $50 \mu\text{m}$ to determine the optimal spacing for a cell design at a TDD of 10^6 cm^{-2} . The influence of variation in the grid finger-pitch on the efficiency (η), V_{oc} , fill-factor (FF) (inset shows J_{sc}), and voltage at the maximum power point (V_m) with increasing concentration under AM1.5 d were plotted in Fig. 3(a)–(d), respectively. It can be clearly seen that our preliminary cell with

TABLE I
DEPENDENCE OF 2-J CELL PERFORMANCE ON FINGER-PITCH AT
TDD $\sim 10^6 \text{ cm}^{-2}$

Grid Finger-Pitch (μm)	V_{oc} (V)	J_{sc} (mA/cm^2)	FF (%)	Efficiency (%)
1-sun				
500 μm	2.356	12.86	86.87	29.29
100 μm	2.358	12.50	86.89	28.44
300-suns				
500 μm	2.681	3859.1	66.94	25.63
100 μm	2.679	3751.13	87.37	32.49

TABLE II
DEPENDENCE OF 2-J CELL EFFICIENCY ON TDD

TDD (cm^{-2})	1-sun AM 1.5 d Efficiency (%)	Peak CPV Efficiency (%) (Peak Concentration) – Optimal Grid Finger-Pitch
10^5	30.73	33.84 (100 x) – 200 μm
10^6	29.29	32.49 (300 x) – 100 μm
10^7	25.88	29.12 (300 x) – 100 μm

a grid finger-pitch of 500 μm demonstrated the best performance under 1 sun. However, with increasing sun concentration, the performance began to degrade with the peak efficiency of 31.71% occurring at merely 50 suns. Due to a wider grid finger-pitch of 500 μm , the effect of series resistance was more pronounced at low concentrations, thus limiting the peak performance to only 50 suns and rendering this cell design inefficient for CPV operation.

From Fig. 3(a), one can clearly find that as the front grid spacing was reduced, the efficiency at 1 sun for the 50- μm finger-pitch dropped significantly due to the lower photon flux reaching the cell as a result of increased grid shadowing. However, the advantage of reducing the front grid spacing was clearly seen at higher concentration, evident by the improvement in efficiency and the extension of peak performance to higher concentration. For the cell with a grid finger-pitch of 50 μm , the low-absorbed photon flux [and the corresponding low J_{sc} , as evident by the inset of Fig. 3(c)], overpowered the benefits gained by minimizing the I^2R resistive losses. The cell with a finger-pitch of 100 μm exhibited the best performance at higher concentration (32.49% at 300 suns). The grid finger-pitch of 100 μm reduced the resistive path, while allowing sufficient photon flux to reach the cell, thus underlining the importance of accurate grid design at an intended-concentrated level. The resulting solar cell performance parameters are compared for the best grid finger-pitch of 100 μm with the preliminary grid finger-pitch of 500 μm in Table I. In addition, to get a clear insight on the dependence of cell performance on the TDD, we simulated 2-J InGaP/GaAs solar cell on Si for CPV operation with TDD varying from 10^5 to 10^7 cm^{-2} , with subcells being current-matched at each respective TDD. The grid finger-pitch design at each respective TDD was optimized and the performance results obtained are summarized in Table II.

From Fig. 3(a), it is also worth noting that even for the optimized 100- μm grid finger-pitch, the efficiency peaked at 300

suns and then eventually decreased thereafter. The solar cell performance parameters (J_{sc} , V_{oc} , J_m , V_m) were analyzed to investigate the root cause of the degradation in performance beyond 300 suns, starting with J_{sc} first. It is evident from the inset of Fig. 3(c) that the J_{sc} continued to increase with sun concentration, irrespective of the finger-pitch and, hence, was not a performance limiting factor. From Fig. 3(b), it can be inferred that the V_{oc} had a logarithmic dependence on the concentration. Assuming constant temperature, V_{oc} under concentrated sunlight can be expressed as [29]

$$V_{oc}^{X\text{ suns}} = V_{oc}^{1\text{ sun}} + n \frac{kT}{q} \ln X \quad (2)$$

where n is the effective diode ideality factor, k is the Boltzman constant, X is the sun concentration, and q is the elementary charge. From Fig. 3(b), one can find that the V_{oc} continued to increase with the concentration and, therefore, was not a factor limiting the cell performance to increase beyond 300 suns. Using (2), the slope of V_{oc} versus logarithmic of concentration was calculated to be $\sim 2.21 \text{ kT}$, close to the predicated value of 2 kT for two series-connected ideal diodes. The higher value of the ideality factor was attributed to the recombination within the base region of the subcells owing to the TDD. We utilized this ideality factor to compute the series resistance, which we discuss in the subsequent Section III-C. While J_{sc} and V_{oc} continued to increase with concentration, it is evident from Fig. 3(c) that the FF was adversely impacted, especially for the cells which had wider grid finger-pitch. The decrease in FF at higher concentration was attributed to the effect of series resistance associated with V_m . We next address in greater details the role of series resistance and the associated I^2R losses in limiting the cell performance at higher concentrations.

C. Role of Series Resistance on the Cell Performance

Among the solar cell parameters (V_m , J_m , V_{oc} , J_{sc}) which influence the FF, we found that all of these parameters continued to increase with concentration, except V_m . Unlike V_{oc} , which increased logarithmically with concentration, V_m had a nonlinear dependence as shown in Fig. 3(d). Thus, the degradation in V_m with increasing concentration limited the cell efficiency to rise beyond a certain concentration due to the impact of both series and shunt resistance. With the increase in concentration, the degradation in V_m was found to be less severe for narrower grid finger-pitch, as evident from Fig. 3(d). This was attributed to the pronounced effect of series resistance for the widely spaced grid fingers owing to a longer resistive path for the electrons to travel before being collected in the gridlines. As a consequence of the degradation in V_m with increasing concentration, the efficiency was most severely impacted for the cell with wider grid finger-pitch, as shown in Fig. 3(a).

The resistive power losses increase with the square of current density, having a stronger impact at higher concentration. The enhanced effect of series resistance with increasing grid finger-pitch is illustrated in the J - V characteristics of the 2-J InGaP/GaAs cell on Si at 300 suns at a TDD of 10^6 cm^{-2} , as shown in Fig. 4(a). In order to gain quantitative insight into the

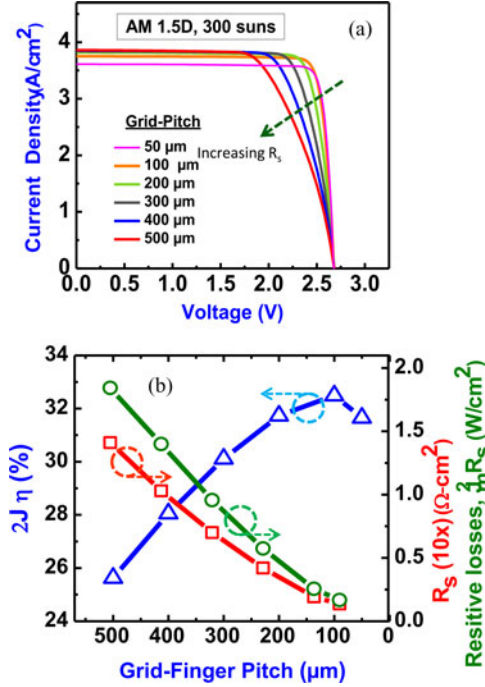


Fig. 4. (a) J - V characteristics of 2-J InGaP/GaAs solar cell on Si (under AM1.5 d, 300 suns) for various grid finger-pitches at a TDD of 10^6 cm^{-2} . (b) 2-J cell η , R_s , and $(J_m)^2 R_s$ resistive losses as a function of grid-finger pitch at a TDD of 10^6 cm^{-2} .

design tradeoffs for optimizing series resistance and shadowing losses at higher concentration, we evaluated the effective series resistance and the associated $I^2 R$ losses at 300 suns. The efficiency of the 2-J InGaP/GaAs cell on Si at 300 suns, the R_s and the associated $(J_m)^2 R_s$ losses are plotted as a function of the variation in grid finger-pitch in Fig. 4(b). One can clearly see that both the R_s and $(J_m)^2 R_s$ resistive losses decrease with the decrease in grid finger-pitch. This facilitated an increase in efficiency for the cells with narrower grid finger-pitch. However, this trend of increase in efficiency with decrease in grid finger-pitch was effective only until the shadowing losses began to dominate and limit the performance. This was evident in the cell with a grid finger-pitch of $50 \mu\text{m}$. Although the $(J_m)^2 R_s$ losses were minimized for grid finger-pitch of $50 \mu\text{m}$, the photon flux reaching the cell was significantly reduced due to the increased shadowing losses, thereby, limiting the cell performance. Thus, the design tradeoffs between shadowing losses and series resistance for CPV operation were best optimized at a grid finger-pitch of $100 \mu\text{m}$.

D. Optimizing of the Doping in the Top Cell Window Layer

The conductivity of the top cell window-emitter layers plays a significant role in extending the peak cell performance toward higher concentration, enabling more efficient design for economical CPV. In a typical n+/p solar cell, the electrons flow laterally in the top cell's window layer before they are collected at the gridlines. This lateral electron flow makes the optimization of the conductivity of the window-emitter layers of key impor-

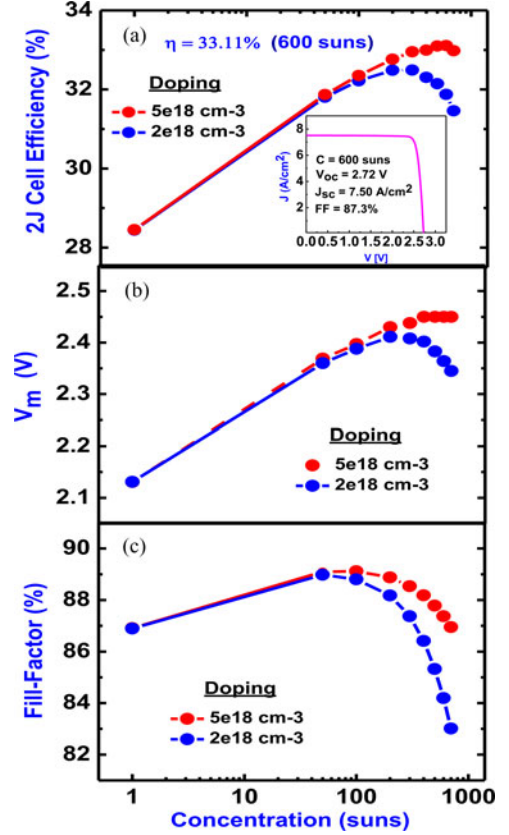


Fig. 5. Impact of doping concentration in the InAlP window layer on the performance of 2-J InGaP/GaAs solar cell on Si at a TDD of 10^6 cm^{-2} : (a) η , (b) V_m , and (c) FF under AM1.5 d. The inset in (a) shows the J - V characteristic of the optimized 2-J InGaP/GaAs solar cell with grid finger-pitch of $100 \mu\text{m}$ and window layer doping concentration of $n = 5 \times 10^{18} \text{ cm}^{-3}$ at 600 suns.

TABLE III
DEPENDENCE OF 2-J CELL EFFICIENCY ON THE WINDOW LAYER DOPING

Doping (cm^{-3})	1-sun Efficiency (%)	Peak Concentration (suns)	Peak Efficiency (%)
2.00×10^{18}	28.44	300	32.49
3.50×10^{18}	28.45	500	32.93
5.00×10^{18}	28.45	600	33.11
8.00×10^{18}	28.46	600	33.23

tance to minimize the $I^2 R$ resistive losses and indeed translates to substantial performance improvement.

Our optimized cell design with a grid finger-pitch of $100 \mu\text{m}$ (from Section III-B), utilized an $\text{In}_{0.5}\text{Al}_{0.5}\text{P}$ window layer with a doping concentration of $n = 2 \times 10^{18} \text{ cm}^{-3}$. In order to optimize the doping concentration in the window layer, we varied it from $n = 2 \times 10^{18} \text{ cm}^{-3}$ to $n = 8 \times 10^{18} \text{ cm}^{-3}$, while keeping the grid finger-pitch fixed at $100 \mu\text{m}$ and taking into account the impact of TDD. The influence of increasing sun concentration on the η , V_m , and FF for the 2-J InGaP/GaAs cell on Si at two different window layer doping concentrations ($n = 2 \times 10^{18} \text{ cm}^{-3}$ and $n = 5 \times 10^{18} \text{ cm}^{-3}$) is illustrated in Fig. 5(a), (b), and (c), respectively, and the key results are summarized in Table III. It is worth noting that as the doping concentration in the

window layer was increased, the peak cell efficiency continued to increase, with the best performance of 33.23% occurring at 600 suns for $n = 8 \times 10^{18} \text{ cm}^{-3}$. However, obtaining a high doping concentration of $n = 8 \times 10^{18} \text{ cm}^{-3}$ in the InAlP window layer can be challenging during material growth. Therefore, we selected a more realistic and achievable doping concentration of $n = 5 \times 10^{18} \text{ cm}^{-3}$. From Fig. 5(a), we can see that by increasing the doping concentration from $n = 2 \times 10^{18} \text{ cm}^{-3}$ to $n = 5 \times 10^{18} \text{ cm}^{-3}$, the peak performance of 32.49% at 300 suns was extended to 33.11% at 600 suns. This improvement in cell performance was attributed to the improvement in V_m and the FF [see Fig. 5(b) and (c)] owing to the reduction in the I^2R resistive losses. Although the gain in cell performance by increasing window layer doping concentration from $n = 2 \times 10^{18} \text{ cm}^{-3}$ to $n = 5 \times 10^{18} \text{ cm}^{-3}$ was only 0.62%, the shift in peak performance from 300 to 600 suns will allow to significantly scale down the cell size and contribute substantially toward cost reduction. The drop in cell performance beyond 600 suns was attributed to the effect of series resistance, emanating from the bulk resistance of the epi-layers. It was not due to the J_{sc} of the 2-J cell exceeding the peak tunneling current density of the TJ at 600 suns, since AlGaAs/GaAs-based TJs have been previously demonstrated with peak tunneling current density in excess of 7.5 A/cm^2 , the J_{sc} of our 2-J InGaP/GaAs cell on Si at 600 suns [30], [31]. Performance prediction of $\sim 33\%$ for 2-J InGaP/GaAs solar cells on Si is encouraging for future research and development of III-V solar cells on Si substrate for CPV application.

IV. CONCLUSION

We have demonstrated a design methodology oriented toward maximizing the performance of 2-J InGaP/GaAs solar cell on Si for concentrated photovoltaics, incorporating TDs. The current-matching condition under AM1.5d was realized at TDD varying from 10^5 to 10^7 cm^{-2} . A theoretical conversion efficiency of 29.29% at a realistic TDD of 10^6 cm^{-2} was achieved for the 2-J InGaP/GaAs solar cell design on Si with a grid finger-pitch of $500 \mu\text{m}$. The bottom GaAs subcell was found to limit the overall performance of the 2-J InGaP/GaAs solar cell on Si.

The design tradeoffs between the losses due to grid shadowing and series resistance were optimized to maximize the performance under higher concentration. At a TDD of 10^6 cm^{-2} , the optimal grid finger-pitch was found to be $100 \mu\text{m}$, demonstrating an efficiency of 32.49% at 300 suns. Increasing the window layer doping from $n = 2 \times 10^{18} \text{ cm}^{-3}$ to $n = 5 \times 10^{18} \text{ cm}^{-3}$ allowed to extend the peak performance to 600 suns, improving the conversion efficiency to 33.11%, a greater than absolute 3.5% performance improvement compared with 1-sun. We have demonstrated the importance of optimizing the cell design for a target concentration at a specific TDD. Our model predicts theoretical conversion efficiency in excess of 33% at 600 suns for 2-J InGaP/GaAs solar cell on Si at a TDD of 10^6 cm^{-2} . The performance results are encouraging and show a promising future for integrating metamorphic III-V concentrator solar cells on Si substrate for CPV applications.

REFERENCES

- [1] G. S. Kinsey, P. Hebert, K. E. Barbour, D. D. Krut, H. L. Cotal, and R. A. Sherif, "Concentrator multijunction solar cell characteristics under variable intensity and temperature," *Prog. Photovoltaics, Res. Appl.*, vol. 16, pp. 503–508, 2008.
- [2] D. Shahjerdi, S. W. Bedell, C. Ebert, C. Bayram, B. Hekmatshoar, K. Fogel, P. Lauro, M. Gaynes, T. Gokmen, J. A. Ott, and D. K. Sadana, "High-efficiency thin-film InGaP/InGaAs/Ge tandem solar cells enabled by controlled spalling technology," *Appl. Phys. Lett.*, vol. 100, pp. 053901–1–053901-3, 2012.
- [3] S. Burroughs, R. Conner, B. Furman, E. Menard, A. Gray, M. Meitl, S. Bonafede, D. Kneeburg, K. Ghosal, R. Bukovnik, W. Wagner, S. Seel, and M. Sullivan, "A new approach for a low cost CPV module design utilizing micro-transfer printing technology," *AIP Conf. Proc.*, vol. 1277, pp. 163–166, 2010.
- [4] R. Tatavarti, A. Wibowo, G. Martin, F. Tuminello, C. Youtsey, G. Hillier, N. Pan, M. W. Wanlass, and M. Romero, "InGaP/GaAs/InGaAs inverted metamorphic (IMM) solar cells on 4" epitaxial lifted off (ELO) wafers," in *Proc. 35th IEEE Photovoltaic Spec. Conf.*, 2010, pp. 002125–002128.
- [5] G. J. Bauhuis, P. Mulder, E. J. Haverkamp, J. J. Schermer, E. Bongers, G. Oomen, W. Köstler, and G. Strobl, "Wafer reuse for repeated growth of III-V solar cells," *Prog. Photovoltaics, Res. Appl.*, vol. 18, pp. 155–159, 2010.
- [6] V. Sabnis, H. Yuen, and M. Wiemer, "High-efficiency multijunction solar cells employing dilute nitrides," *AIP Conf. Proc.*, vol. 1477, pp. 14–19, 2012.
- [7] J. F. Geisz, S. Kurtz, M. W. Wanlass, J. S. Ward, A. Duda, D. J. Friedman, J. M. Olson, W. E. McMahon, T. E. Moriarty, and J. T. Kiehl, "High-efficiency GaInP/GaAs/InGaAs triple-junction solar cells grown inverted with a metamorphic bottom junction," *Appl. Phys. Lett.*, vol. 91, pp. 023502–1–023502-3, 2007.
- [8] N. Jain and M. K. Hudait, "Design of metamorphic dual-junction InGaP/GaAs solar cell on Si with efficiency greater than 29% using finite element analysis," in *Proc. 38th IEEE Photovoltaic Spec. Conf.*, 2012, pp. 002056–002060.
- [9] N. Jain and M. K. Hudait, "Impact of threading dislocations on the design of GaAs and InGaP/GaAs solar cells on Si using finite element analysis," *IEEE J. Photovoltaics*, vol. 3, no. 1, pp. 528–534, Jan. 2013.
- [10] R. R. King, D. C. Law, K. M. Edmondson, C. M. Fetzer, G. S. Kinsey, H. Yoon, R. A. Sherif, and N. H. Karam, "40% efficient metamorphic GaInP/GaInAs/Ge multijunction solar cells," *Appl. Phys. Lett.*, vol. 90, pp. 183516–1–183516-3, 2007.
- [11] W. Guter, J. Schone, S. Philipps, M. Steiner, G. Siefer, A. Wekkeli, E. Welsler, E. Oliva, A. W. Bett, and F. Dimroth, "Current-matched triple-junction solar cell reaching 41.1% conversion efficiency under concentrated sunlight," *Appl. Phys. Lett.*, vol. 94, pp. 223504–1–223504-3, 2009.
- [12] M. R. Lueck, C. L. Andre, A. J. Pitera, M. L. Lee, E. A. Fitzgerald, and S. A. Ringel, "Dual junction GaInP/GaAs solar cells grown on metamorphic SiGe/Si substrates with high open circuit voltage," *IEEE Electron Device Lett.*, vol. 27, no. 3, pp. 142–144, Mar. 2006.
- [13] APSYS, *Advanced Physical Models of Semiconductor Devices*, Crosslight Software Inc., Burnaby, BC, Canada.
- [14] D. J. Friedman, "Modeling of tandem cell temperature coefficients," in *Proc. 25th IEEE Photovoltaic Spec. Conf.*, 1996, pp. 89–92.
- [15] M. Yamaguchi, C. Amano, and Y. Itoh, "Numerical-analysis for high-efficiency GaAs solar-cells fabricated on Si substrate," *J. Appl. Phys.*, vol. 66, pp. 915–919, 1989.
- [16] C. L. Andre, J. J. Boeckl, D. M. Wilt, A. J. Pitera, M. L. Lee, E. A. Fitzgerald, B. M. Keyes, and S. A. Ringel, "Impact of dislocations on minority carrier electron and hole lifetimes in GaAs grown on metamorphic SiGe substrates," *Appl. Phys. Lett.*, vol. 84, pp. 3447–3449, 2004.
- [17] M. L. Lovejoy, M. R. Melloch, and M. S. Lundstrom, "Minority hole mobility in GaAs," in *Properties of Gallium Arsenide*, M. R. Brozel and G. E. Stillman, Eds. London, U.K.: INSPEC, 1996, pp. 123–130.
- [18] R. K. Ahrenkiel and M. S. Lundstrom, "Minority carrier transport in III-V semiconductors," in *Minority Carrier in III-V Semiconductors: Physics and Applications (Semiconductors and Semimetals)*, vol. 39. R. K. Willardson, A. C. Beer, and E. R. Weber, Eds. New York, NY, USA: Academic, 1993, pp. 193–258.
- [19] M. Y. Ghannam, J. Poortmans, J. F. Nijs, and R. P. Mertens, "Theoretical study of the impact of bulk and interface recombination on the performance of GaInP/GaAs/Ge triple junction tandem solar cells," in *Proc. 3rd World Conf. Photovoltaic Energy Convers.*, 2003, pp. 666–669.

- [20] T. Takamoto, M. Yamaguchi, S. J. Taylor, M.-J. Yang, E. Ikeda, and H. Kurita, "Radiation resistance of high efficiency InGaP GaAs tandem solar cells," *Sol. Energy Mater. Sol. Cells*, vol. 58, pp. 265–276, 1999.
- [21] T. Takamoto, E. Ikeda, H. Kurita, and M. Ohmori, "Structural optimization for single junction InGaP solar cell," *Sol. Energy Mater. Sol. Cells*, vol. 35, pp. 25–31, 1994.
- [22] I. Garcia, I. Rey-Stolle, B. Galiana, and C. Algora, "A 32.6% efficient lattice-matched dual-junction solar cell working at 1000 suns," *Appl. Phys. Lett.*, vol. 94, pp. 053509-1–053509-3, 2009.
- [23] M. Steiner, S. P. Philipps, M. Hermle, A. W. Bett, and F. Dimroth, "Validated front contact grid simulation for GaAs solar cells under concentrated sunlight," *Prog. Photovoltaics, Res. Appl.*, vol. 19, pp. 73–83, 2011.
- [24] G. L. Araujo and E. Sanchez, "A new method for experimental determination of the series resistance of a solar cell," *IEEE Trans. Electron Devices*, vol. ED-29, no. 10, pp. 1511–1513, Oct. 1982.
- [25] A. G. Aberle, S. R. Wenham, and M. A. Green, "A new method for accurate measurements of the lumped series resistance of solar cells," in *Proc. 23rd IEEE Photovoltaic Spec. Conf.*, 1993, pp. 133–139.
- [26] K. Rajkanan and J. Shewchun, "A better approach to the evaluation of the series resistance of solar cells," *Solid State Electron.*, vol. 22, pp. 193–197, 1979.
- [27] M. Wolf and H. Rauschenbach, "Series resistance effects on solar cell measurements," *Adv. Energy Convers.*, vol. 3, pp. 455–479, 1963.
- [28] A. R. Moore, "An optimized grid design for a sun-concentrator solar cell," *RCA Rev.*, vol. 40, pp. 140–152, 1979.
- [29] C. Algora, "The importance of the very high concentration in third-generation solar cells," in *Next Generation Photovoltaics*, A. Marti and A. Luque, Eds. Boca Raton, FL, USA: CRC, 2004, pp. 108–139.
- [30] S. Wojtczuk, P. Chiu, Z. Xuebing, D. Derkacs, C. Harris, D. Pulver, and M. Timmons, "InGaP/GaAs/InGaAs 41% concentrator cells using bi-facial epi-growth," in *Proc. 35th IEEE Photovoltaic Spec. Conf.*, 2010, pp. 1259–1264.
- [31] J. F. Wheeldon, C. E. Valdivia, A. W. Walker, G. Kolhatkar, A. Jaouad, A. Turala, B. Riel, D. Masson, N. Puetz, S. Fafard, R. Arès, V. Aimez, T. J. Hall, and K. Hinzer, "Performance comparison of AlGaAs, GaAs and InGaP tunnel junctions for concentrated multijunction solar cells," *Prog. Photovoltaics, Res. Appl.*, vol. 19, pp. 442–452, 2011.



Mantu K. Hudait (M'08–SM'08) received the M.S. degree in materials science and engineering from the Indian Institute of Technology, Kharagpur, India, and the Ph.D. degree in materials science and engineering from Indian Institute of Science, Bangalore, India, in 1999.

From 2000 to 2005, he was a Postdoctoral Researcher with the Ohio State University, Columbus, OH, USA, and worked on the mixed cation and mixed anion metamorphic graded buffer, carrier transport in mixed anion systems, low-bandgap thermophotovoltaics, and heterogeneous integration of III–V solar cells on Si using a SiGe buffer. From 2005 to 2009, he was a Senior Engineer with the Advanced Transistor and Nanotechnology Group, Intel Corporation. His breakthrough research in low-power transistor on Si at Intel Corporation was press released in 2007 and 2009. In 2009, he joined the Bradley Department of Electrical and Computer Engineering, Virginia Tech, Blacksburg, VA, USA, as an Associate Professor. He has more than 137 technical publications and refereed conference proceedings and holds 45 U.S. patents. His current research at Virginia Tech focuses on the heterogeneous integration of compound semiconductors and Ge on Si for ultralow power logic and photovoltaics. His research interests include III–V compound semiconductor epitaxy, defect engineering in nanoscale, metamorphic buffers, and devices for sustainable energy-related applications, including thermophotovoltaics and III–V and Ge quantum well and tunnel FETs.

Dr. Hudait received two Divisional Recognition Awards from Intel Corporation. He is a Member of American Vacuum Society and the American Society for Engineering Education.



Nikhil Jain (S'12) received the B.S. degree (Hons.) in electrical and computer engineering from the University of Illinois, Champaign, IL, USA, in 2010, and is currently working toward the Ph.D. degree with the Bradley Department of Electrical Engineering, Virginia Tech, Blacksburg, VA, USA.

His research interests include design and modeling, epitaxial growth and fabrication of compound semiconductors, and Ge-based materials and devices for sustainable energy and low-power transistor applications. His current research interest includes the

heterogeneous epitaxy of III–V multijunction solar cells on Si via molecular beam epitaxy.

Mr. Jain received the Paul E. Torgersen Award, the John Bardeen Award, and the ISSS Undergraduate Scholarship while at the University of Illinois. He was nominated as a finalist for the Best Student Poster Award at the 38th IEEE Photovoltaic Specialists Conference and served as the Graduate Student Assistant at the 40th IEEE Photovoltaic Specialists Conference.